Optocoupler Pulse and Digital Circuits

Elena Koleva[1] and Ivan Kolev[2]

Abstract – **The advantages of introducing the optocouplers into the pulse and digital circuits are as follows: additional control inputs, galvanic separation of the control signals by the circuit, higher noise immunity, current control inputs, etc.**

Keywords – **Optocoupler Pulse circuit, Optocoupler Digital circuit.**

I. INTRODUCTION

Common pulse and digital circuits are usually realized by means of one optocoupler. In our case the two active elements in these circuits are suggested to be replaced by optocouplers.

II. PULSE CIRCUITS

A. Schmitt trigger – fig. 1.

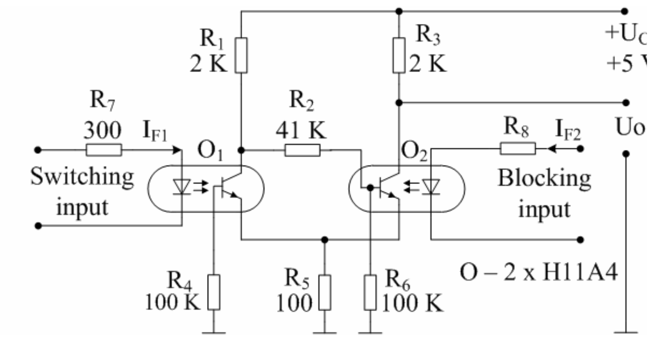

Fig. 1. Schmitt trigger

The input I_{F1} is controlling and the input I_{F2} is blocking.
In order for the Schmitt trigger to normally operate, it is required that $I_{F2} = 0$.

In order for the Schmitt trigger to switch, the following conditions must be fulfilled – Eq. 1:

$$I_{F1on} > \frac{U_{CC} - U_{CEsat1}}{K_{i1}.R_1} + \frac{U_{CC}}{R_3 + R_5}.\frac{R_5}{R_4}.\frac{h_{21E1}}{K_{i1}} \qquad (1)$$

where K_{i1} – the current transmission coefficient of the phototransistor optocoupler O_1, h_{21E1} – the current amplification factor of the phototransistor optocoupler O_1, U_{CEsat1} – the voltage between the collector and the emitter of the phototransistor optocoupler O_1 in a saturation mode.

For example $K_{i1} = 0{,}2$ ($R_4 = 100$ kΩ), $U_{CEsat1} = 0{,}5$ V, $h_{21E1} = 100$, $I_{F1on} > 12{,}4$ mA.

To keep the blocking of the Schmitt trigger, the following condition should be fulfilled – Eq. 2:

$$I_{F2} > \frac{U_{CC} - U_{CEsat2}}{K_{i2}.R_3} + \frac{U_{CC} - U_{BEsat2}}{R_1 + R_2}.h_{21E2} \qquad (2)$$

e.g. $U_{CEsat2} = 0{,}5$ V, $K_{i2} = 0{,}2$ from expression (2) $I_{F2} > 20$ mA.

B. Monostable multivibrator – fig. 2.

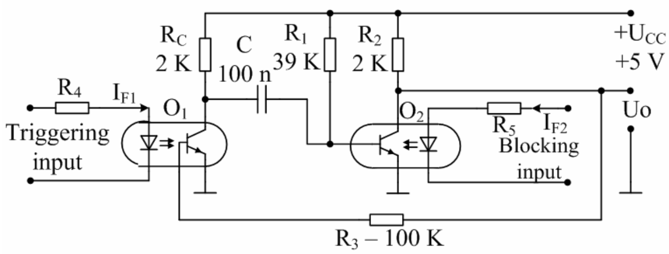

Fig. 2. Monostable multivibrator

Input I_{F1} is triggering and input I_{F2} is blocking. To overturn the monostable multivibrator, the following is required – Eq. 3:

$$I_{F1} > \frac{U_{CC} - U_{CEsat1}}{K_{i1}.R_C} \qquad (3)$$

To block the switching of the monostable multivibrator, the following is required – Eq. 4:

$$I_{F2} > \frac{U_{CC} - U_{CEsat2}}{K_{i2}.R_C} \qquad (4)$$

The output pulse duration of the monostable multivibrator is Eq. 5:

$$t_I \approx 0{,}7.R_1.C; \quad t_I \approx 2{,}7 \text{ ms} \qquad (5)$$

The reset time of the monostable multivibrator is Eq. 6:

$$t_B \approx 3.R_C.C; \quad t_B \approx 600\ \mu s \qquad (6)$$

C. Autofluctuating multivibrator. Simulation of Autofluctoation multivibrator with photodiode optocouplers with PSPICE package.

The time-setting resistors of the autofluctuating multivibrator are replaced by the photodiodes of the optocouplers O_3 and O_4.

The period of pulse repetition is Eq. 7:

[1]Elena Koleva is Ph. D. in the Department of Electronics at Technical University of Gabrovo, H. Dimitar N 4, Gabrovo 5300, Bulgaria, E-mail: elena_ndpt@yahoo.com.

[2]Ivan Kolev is Prof. Dr. Science in the Department of Electronics at Technical University of Gabrovo, H. Dimitar N 4, Gabrovo 5300, Bulgaria, E-mail: ipk_kolev@yahoo.com.

$$T \approx 0,7.C\left[R_{PD3}.(I_{F3}).n_1(I_{F2})+R_{PD4}.(I_{F4}).n_2(I_{F1})\right] \quad (7)$$

$$C_1 = C_2 = C,\ I_{F3} = I_{F4} = I_F,\ R_{PD1} = R_{PD2} = R_{PD}$$

where R_{PD} (I_F) – the resistance of the photodiodes of the optocouplers O_3 and O_4, n_1, n_2 – constants depending on the degree of saturation of the phototransistors of the optocouplers O_1 and O_2 ($n = 1 \div 1,15$).

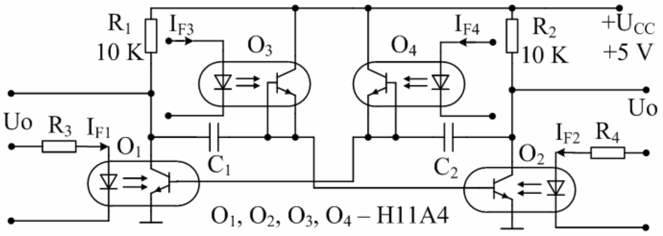

Fig. 3. Autofluctoating multivibrator

By means of the currents of the LEDs I_{F3} and I_{F4}, the period T can be adjusted over 50 times, $n_1 = n_2 = 1,1$; $R_{PD} = 130$ kΩ, $I_F = 30$ mA, T = 20 ms (f = 50 Hz); $R_{PD} = 0,640$ MΩ, $I_F = 0,2$ mA; C = 100 nF, T ≈ 0,98 s (f ≈ 1 Hz).

A traditional circuit of a transistor autofluctuation multivibrator (AMV) has been used, where the transistors have been replaced with phototransistor optocouplers in a photodiode mode, and the base time-setting resistors with optocoupler photodiodes – fig. 3.

The simulated time diagrams of the output voltage U_O (p. 1) and the voltage of one of the time-setting capacitor C_1 (p. 2) are shown in fig. 4.

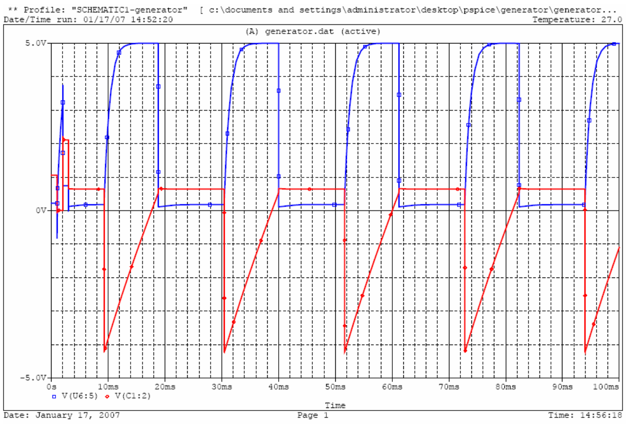

Fig. 4. The simulated time diagrams

The simulation refers to the following case:
$I_{F3} = I_{F4} = 30$ mA, $I_{F1} = I_{F2} = 0$ mA.

The reported simulated period of the generated pulses shown in fig. 4 is $T_{(simulated)} \approx 21$ms.

The equation for the period of the generated pulses, which has been theoretically worked out (Eq. 7).

When $I_{F3} = I_{F4} = 30$ mA, $I_{F1} = I_{F2} = 0$ mA, n_1, $n_2 = 1$, T = 20 ms, f = 50 Hz from Eq. 7.

The error is Eq. 8:

$$\varepsilon = \frac{T_{(simulated)} - T_{(calculated)}}{T_{(simulated)}}.100\,\% = \frac{21-20}{20}.100\% = 5\,\% \quad (8)$$

When $I_{F3} = I_{F4} = 0,2$ mA, $T_И = 0,98$ ms, f ≈ 1 Hz from equation (1), i.e. the frequency changes over approximately 50.

Using table 1, a transfer characteristic of the Autofluctoation multivibrator has been worked out (see fig. 5).

It can be seen that the transfer characteristic is linear within the range $I_F = 5 \div 30$ mA.

TABLE I

I_F, mA	0,2	1	3	5	10
T, ms	960	185	87	64	42
F, Hz	1,04	5,41	11,5	15,6	23,8

I_F, mA	15	20	25	30
T, ms	31	25	21	18
F, Hz	32,3	40	48	55,6

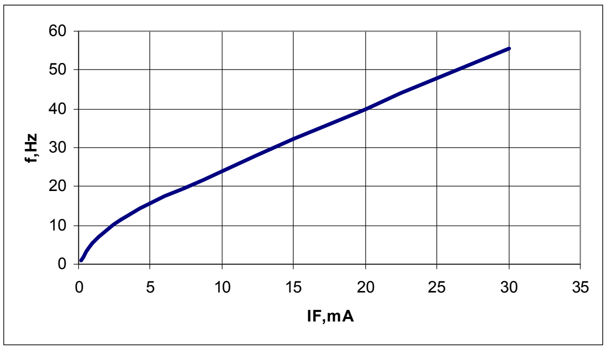

Fig. 5. A transfer characteristic of the Autofluctuation multivibrator

D. Optoelectronic Fantastron generator. Simulation of Optoelectronic Fantastron generator with PSPICE package.

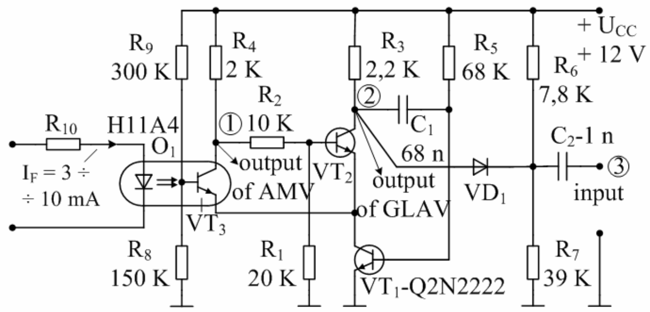

Fig. 6. Optoelectronic Fantastron generator

It operates in a stand-by mode. The transistor fantastron generator has a collector coupling. The generator has an amplifier tracking coupling and contains a generator of line altering negative feedback voltage – Miller integrator with transistors VT_1 and VT_2. The transistors VT_2 and VT_3 form a trigger with an emitter coupling where the emitter resistor is replaced with the transistor VT_1 of the optocoupler O_1.

The circuit simulation is shown in fig. 7.

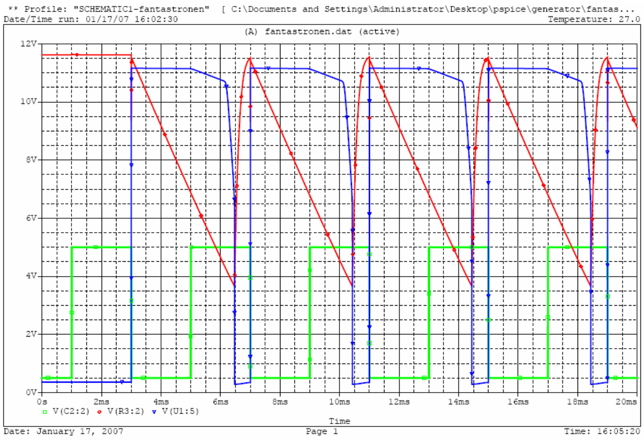

Fig. 7. Simulation of Optoelectronic Fantastron generator

Square pulses are taken at the output p. 1 and line altering voltage at the output p. 2. The circuit is set into motion at input p. 3 by symmetric square pulses of 5 V amplitude and T = 4 ms (f = 250 Hz) period, where the T period of the generator of line altering voltage (GLAV) can be regulated within the range from 3,4 to 2,8 ms by changing the LED current from 3 ÷ 10 mA. The period of simulations is T_C = 4 ms when I_F = 3 mA (fig. 7).

Circuit application:

- Generator of line altering voltage
- Square pulse generator
- Pulse-width modulator
- Time-to-current (voltage) converter

The equations for the pulse duration (t_p), the pause between pulses (t_b), the non-linearity (K_N), controlled voltage (U_C), supply voltage (U_{CC}) and the period T of the generator are – Eq. 9, Eq. 10, Eq. 11, Eq. 12, and Eq. 13:

$$t_p = R_5.C_1\frac{U_{CC}-U_{OL\,GLAV}}{U_{on\,GLAV}} = 68.10^3.68.10^{-9}\,\frac{12-3}{11,5} = 3,62\ ms \qquad (9)$$

$$t_b = R_3.C_1.\ln\frac{U_{CC}}{U_{CC}-U_Y}\,2,2.10^3.68.10^{-9}\,\ln\frac{12}{12-10} = 0,268\,ms \qquad (10)$$

$$U_C = \frac{U_{CC}}{R_6+R_7}.R_7 = \frac{12}{7,8+39}.39 \approx 10\,V \qquad (11)$$

$$T = t_b + t_p = 3,62\,ms + 0,268\,ms = 0,388\,ms \qquad (12)$$

$$K_N = \frac{U_C-U_{OL}}{U_{CC}}.\frac{R_5}{R_3.h_{21E}} = \frac{10-3}{12}.\frac{68}{2,2.180} = 0,1 \qquad (13)$$

The non-linearity of the generator of line altering voltage is K_N = 10 %.

The error, when T = 4 ms, is Eq. 14:

$$\varepsilon = \frac{T_{(simulated)}-T_{(calculated)}}{T_{(simulated)}}.100\,\% = \frac{4-3,88}{4}.100\,\% = 3\% \qquad (14)$$

III. Digital circuits

A. RS – trigger – fig. 8.

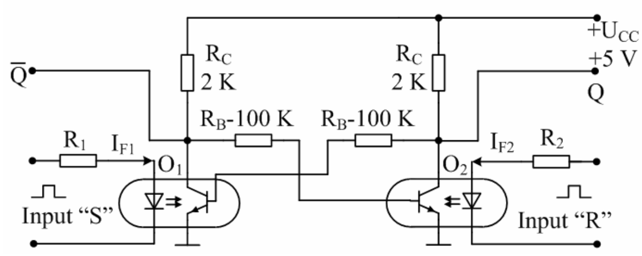

Fig. 8. RS – trigger

This trigger differs from the common ones – there is not an emitter connection (emitter-resistor).

To switch the RS trigger at input S (R), the following is required – Eq. 15:

$$I_F \geq \frac{U_{CC}-U_{CEsat}}{R_C.K_i} \qquad (15)$$

The condition of saturating the phototransistor of the optocouplers can be worked out – Eq. 16, Eq. 17 and Eq. 18:

$$I_B = \frac{U_{CC}-U_{BEsat}}{R_C+R_B} \qquad (16)$$

$$I_C = \frac{U_{CC}-U_{CEsat}}{R_C} \qquad (17)$$

$$I_B \geq \frac{I_C}{h_{21E}} \qquad (18)$$

From the expressions (16), (17) and (18) the following is obtained – Eq. 19:

$$R_B \leq R_C\left(\frac{U_{CC}-U_{BEsat}}{U_{CC}-U_{CEsat}}.h_{21E}-1\right) \qquad (19)$$

Taking into consideration – Eq. 20 and Eq. 21:

$$U_{BEsat} \approx U_{CEsat};\ U_{CC} >> U_{BEsat};\ U_{CC} >> U_{CEsat};\ h_{21E} >>1 \qquad (20)$$

$$R_B < R_C.h_{21E} \qquad (21)$$

IV. Conclusion

Unlike common circuits the input signals here are not voltage but current ones. This results in higher noise immunity of circuits. All input starting, control and blocking signals are galvanically separated by a pulse circuit.

Optoelectronic pulse circuits have been developed. They have been simulated by means of a PSPICE package. Methods for calculating the basic parameters have been elaborated. The circuits have been developed in practice. The simulation and calculation error has been determined – it does not exceed 5 %.

References

[1] Ермаков, О. М. *Прикладная оптоэлектроника.* М. Техносфера, 2004.

[2] Колев, И. С. и Е. Н. Колева. *Инфрачервена оптоелектроника.* Габрово, Унив. изд. „В. Априлов", 2008.

[3] Hewlet Packard. *Optoelectronics Designer's Catalog*, 2000.

[4] OSRAM. *Optosemiconductors*, 2001.